Supplementary Information

Metallic cobalt nanoparticles embedded in sulfur and nitrogen co-doped rambutan-like nanocarbons for oxygen reduction reaction under both acidic and alkaline conditions

Jinyuan Liu[a], Li Xu[a], Yilin Deng[a], Xingwang Zhu[a], Jiujun Deng[a], Jiabiao Lian[a], Jingjie Wu[b], Junchao Qian[c], Hui Xu[a]*, Shouqi Yuan[a], Huaming Li[a]* and Pulickel M. Ajayan[d]

[a] Institute for Energy Research, School of the Environment and Safety Engineering, Jiangsu University, Zhenjiang 212013, P. R. China.

[b] Department of Chemical and Environmental Engineering, University of Cincinnati, Cincinnati, OH 45221, USA.

[c] Jiangsu Key Laboratory for Environment Functional Materials, Suzhou University of Science and Technology, Suzhou 215009, P. R. China.

[d] Department of Materials Science and Nano Engineering, Rice University, Houston, Texas 77005, USA.

***Corresponding author:** Tel.:+86-0511-88799500; Fax: +86-0511-88799500;*

E-mail address: xh@ujs.edu.cn; lihm@ujs.edu.cn

Experimental Section

Chemicals.

All the reagents were of analytical grade and used without further purification.Cobalt acetate tetrahydrate ($(CH_3COO)_2Co{\cdot}4H_2O$, 99% purity), melemine ($C_3H_5N_6$, 99% purity), ethanol (CH_3CH_2OH, 99% purity), tetraethyl orthosilicate (TEOS, 99% purity), sublimed sulfur, Resorcinol and formaldehyde (37 wt %) were purchased from Sinopharm Chemical Reagent Co. Ltd. (China). The Pt catalyst (20 wt%, Pt/C) was purchased from Alfa Aesar Chemicals Co., Ltd. Nafion (10 %) was obtained from Sigma-Aldrich (Missouri, USA). All the solutions used in the experiments were freshly prepared using ultrapure water (Nanjing Baocheng Biotechnology Co. Ltd.,

China).

Material characterization

The crystalline structures of Co@SN-hollow mesoporous carbon sphere and the reference samples were characterized by x-ray diffraction (XRD) using a Shimadzu XRD-6000 diffractometer with Cu Kα radiation across the 2θ range of from 10–80°. X-ray photoelectron spectroscopy (XPS) analysis was performed using a VG MultiLab 2000 system with a monochromatic Mg-Kα line source (20 kV). Brunauer-Emmett-Teller (BET) surface areas were determined by N_2 adsorption and desorption isotherms at 77 K, using a TriStar II 3020 system. The as-prepared catalytst morphologies of as-prepared catalysts were characterized using transmission electron microscopy (TEM) (JEOL JEM-2010 microscope) at an accelerating voltage of 200 kV. Scanning electron microscopy (SEM) observations were performed using a JEOL JSM-7001F microscopy coupled to on energy-dispersive x-ray detector. Raman spectra of the as-prepared catalysts were recorded using a Renishaw spectrometer using a 532 nm laser as an excitation source.

Supplementary Figures:

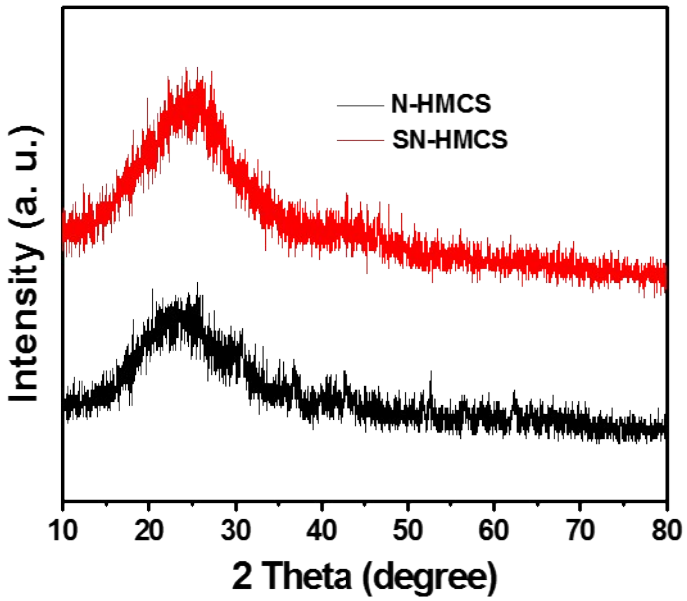

Figure S1. The XRD spectra of N-HMCS and SN-HMCS. Hollow-mesoporous carbon sphere (HMCS).

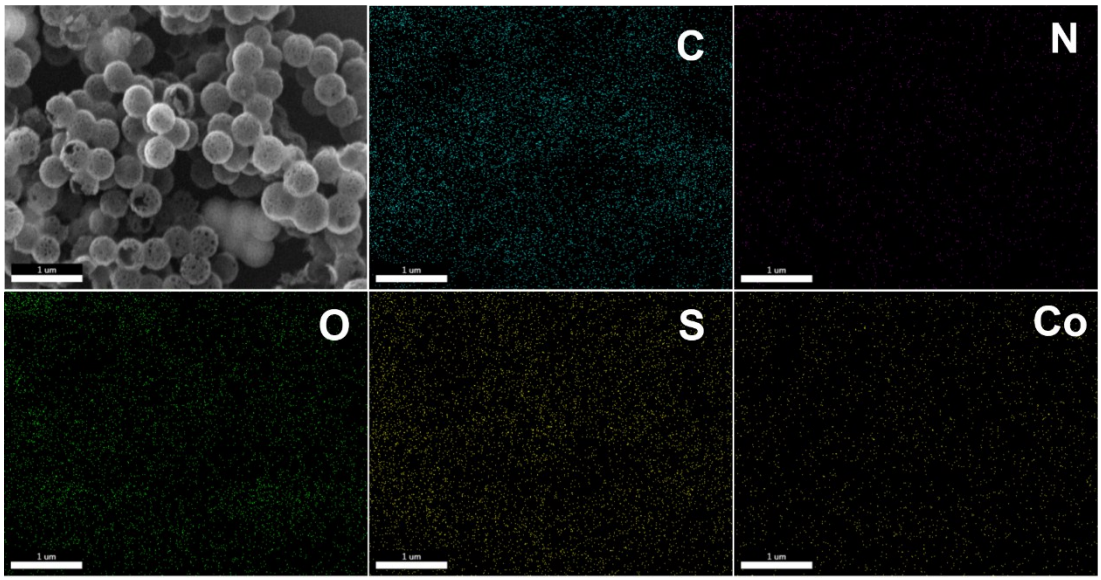

Figure S2. Scanning electron microscopy (SEM) mappings of the Co@SN-HMCS catalyst.

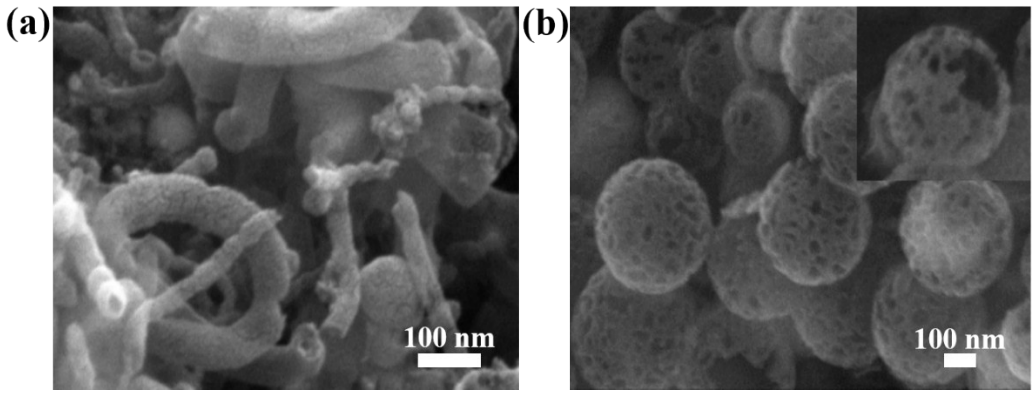

Figure S3. SEM images of the (a) Co@SN-CNT and (b) Co@SN-HMCS catalysts.

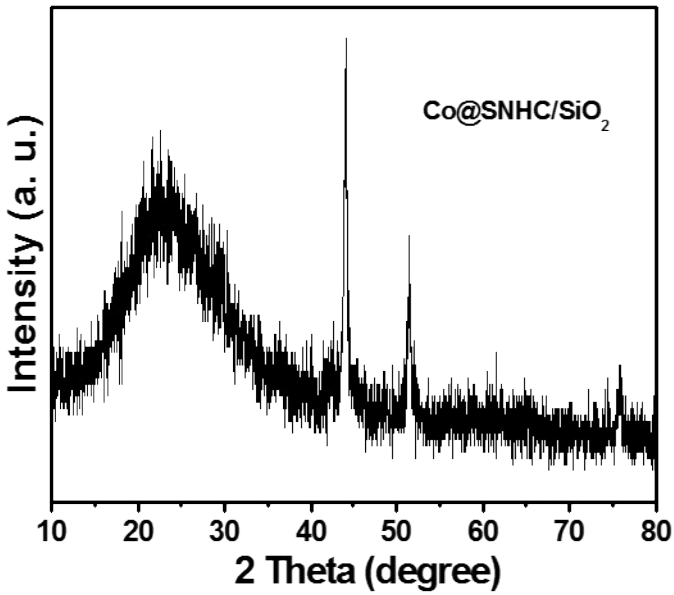

Figure S4. XRD spectra of Co@SNHC/SiO_2 electrocatalyst.

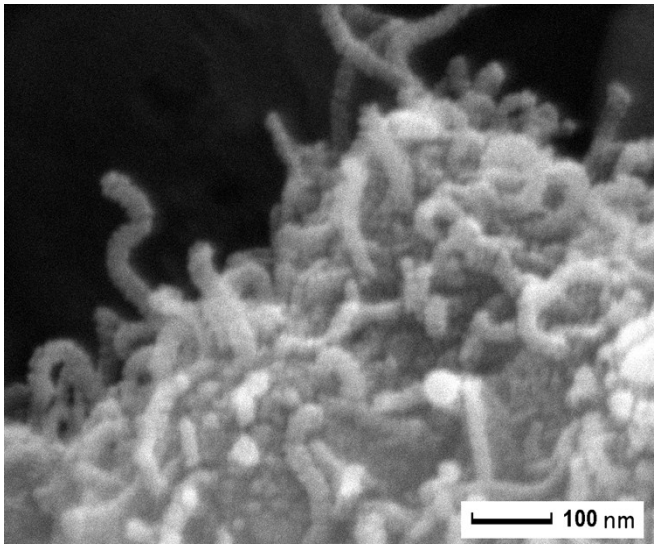

Figure S5. SEM image of Co@NHC. Hierarchical carbon (HC).

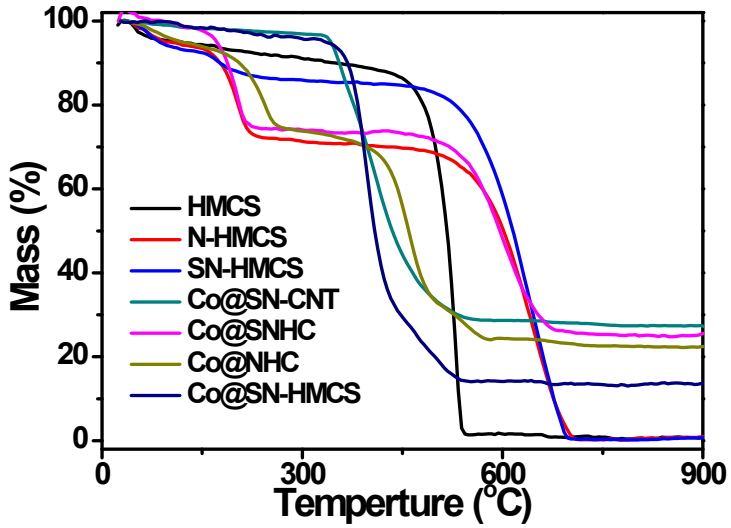

Figure S6. TG thermograms for the as-synthesized catalysts.

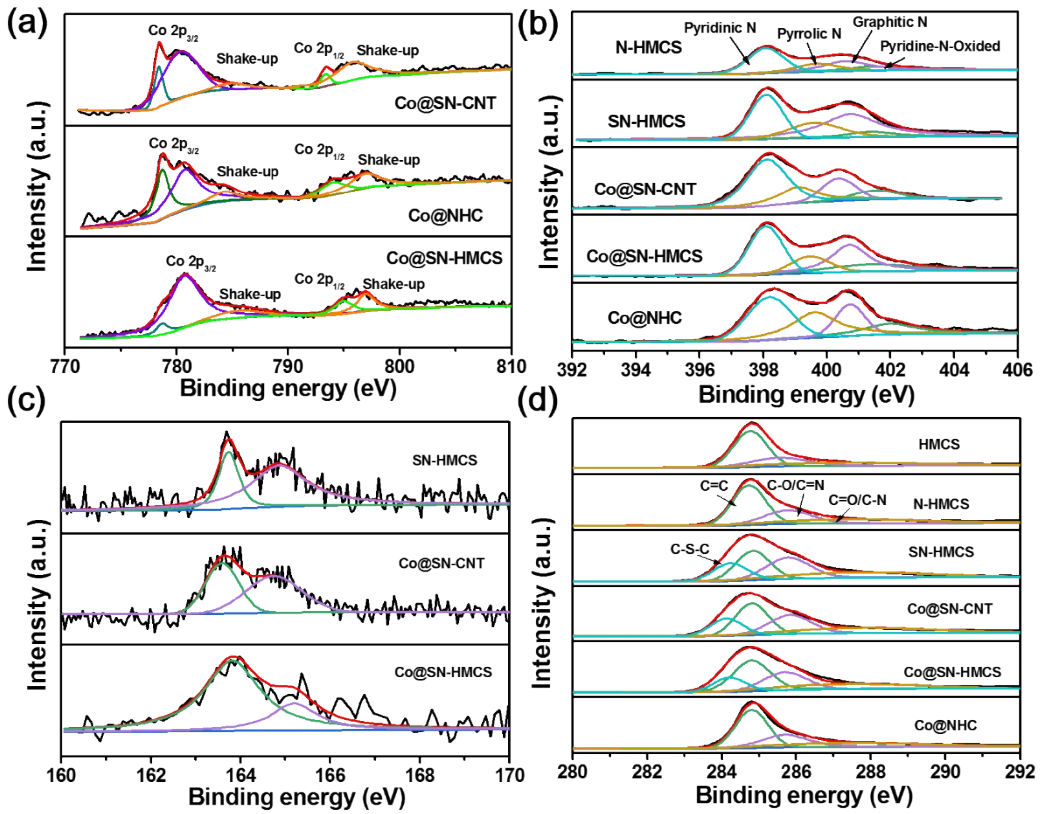

Figure S7. The high-resolution XPS spectra of Co 2p (a), N 1s (b), S 2p (c) and C 1s (d).

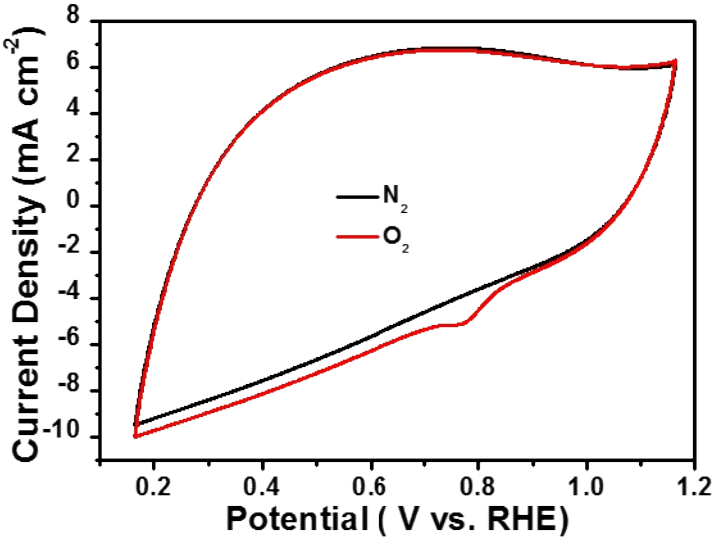

Figure S8. Cyclic voltammetry (CV) curves of Co@SNHC in alkaline conditions.

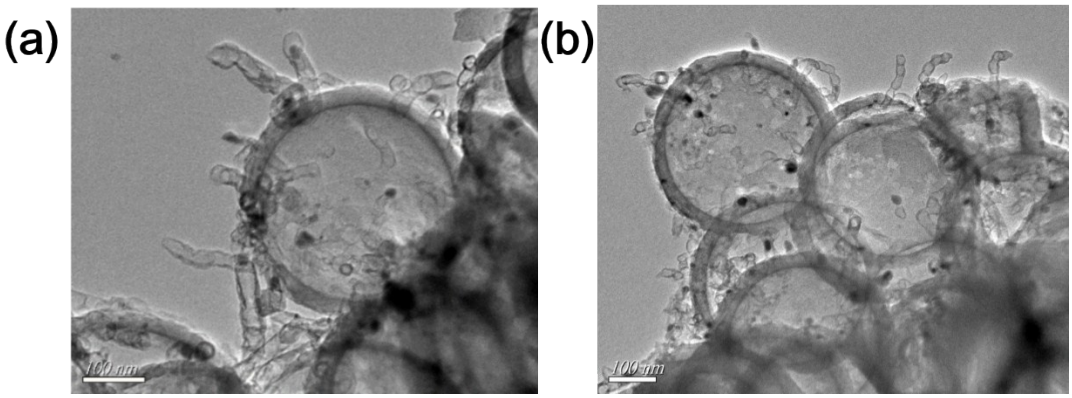

Figure S9. Transmission electron microscopy images of Co@SNHC after 3,000 CV cycles.

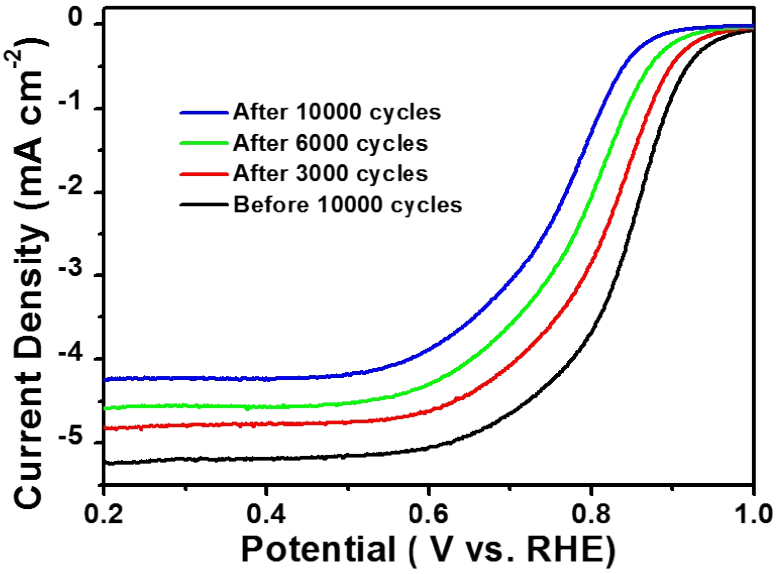

Figure S10. LSV polarization curves (1,600 rpm) of Pt/C before and after 3,000, 6,000 and 10,000 cycles in 0.1 M KOH.

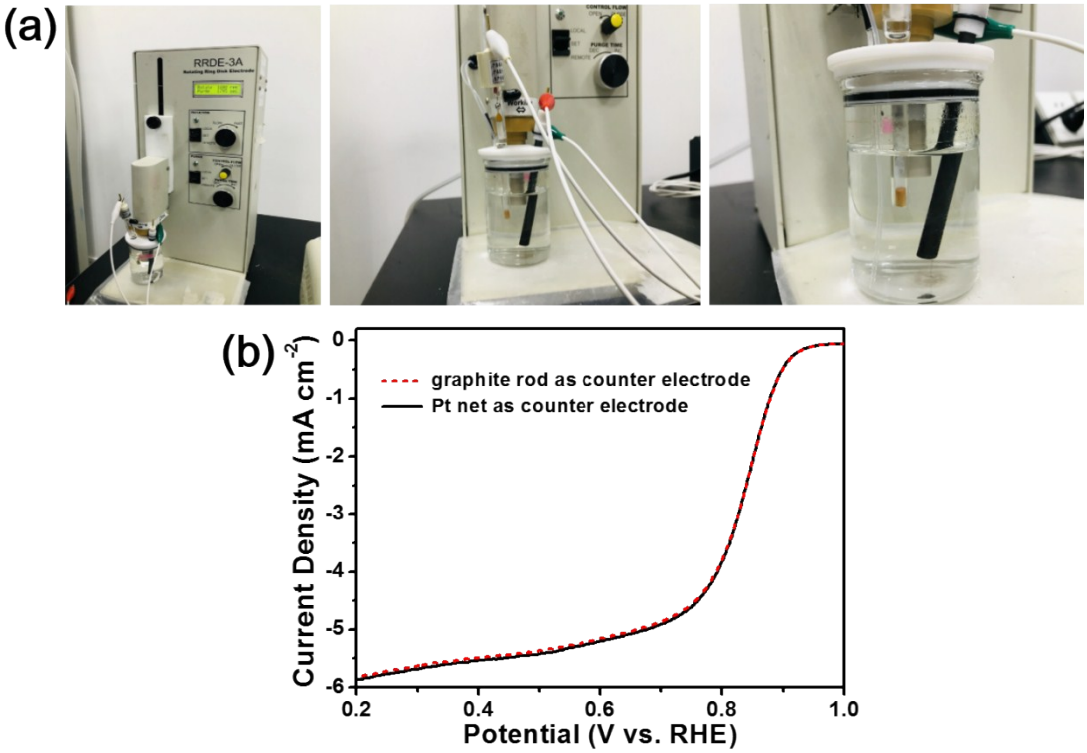

Figure S11. (a) A digital photograph of the experiment setup (RRDE-3A). (b) The ORR polarization curves of Co@SNHC electrocatalyst (Pt net/graphite rod as counter electrode) in 0.1 M KOH condition.

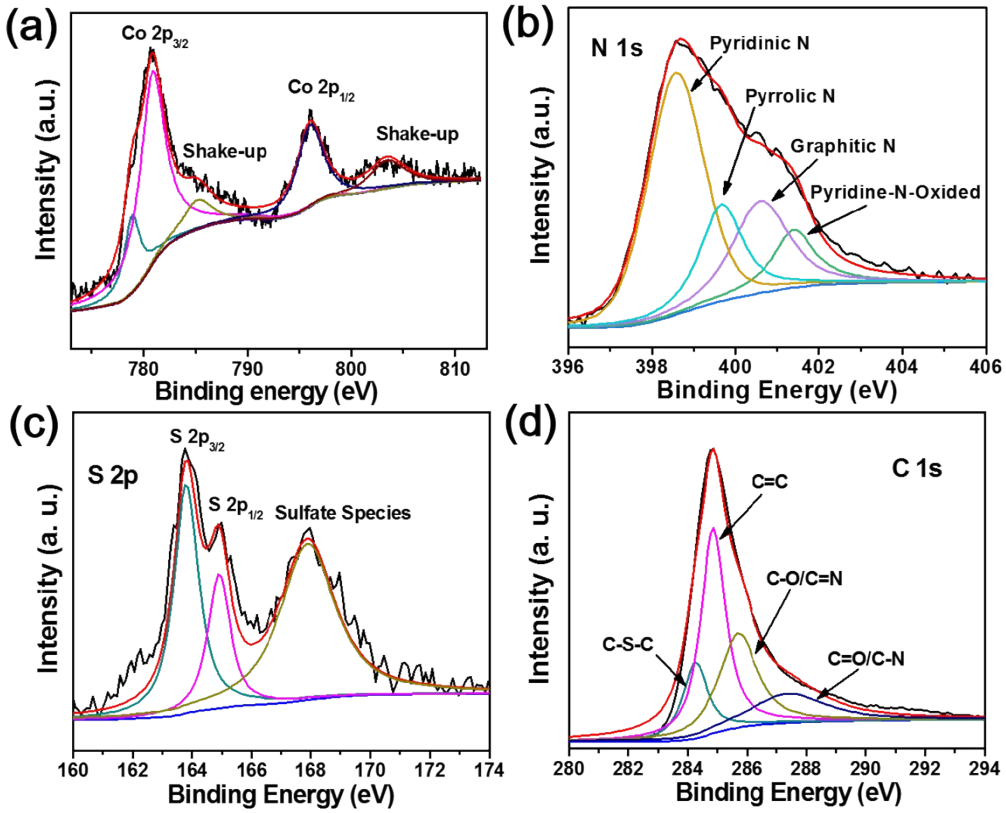

Figure S12. The high resolution XPS spectra for Co 2p (a), N 1s (b), S 2p (c) and C 1s (d) of Co@SNHC electrocatalyst after 30,000 s chronoamperometric response.

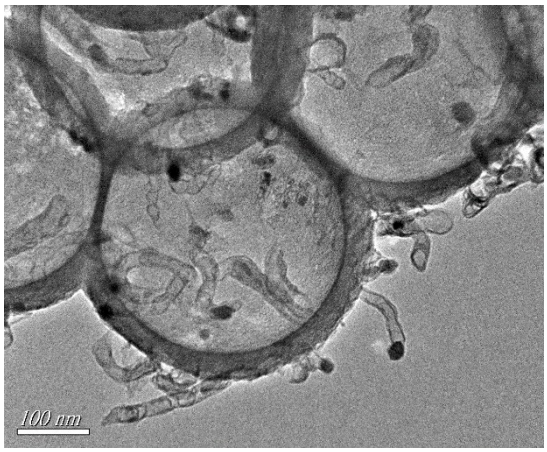

Figure S13. Representative TEM image of Co@SNHC catalyst after 30,000 s chronoamperometric response.

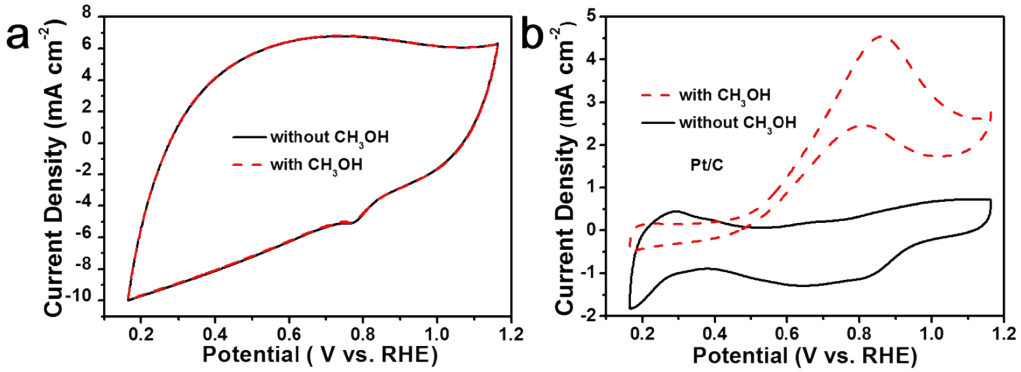

Figure S14. CV polarization curves of (a) Co@SNHC and (b) Pt/C in O_2-saturated 0.1 M KOH solution with or without 1 M CH_3OH.

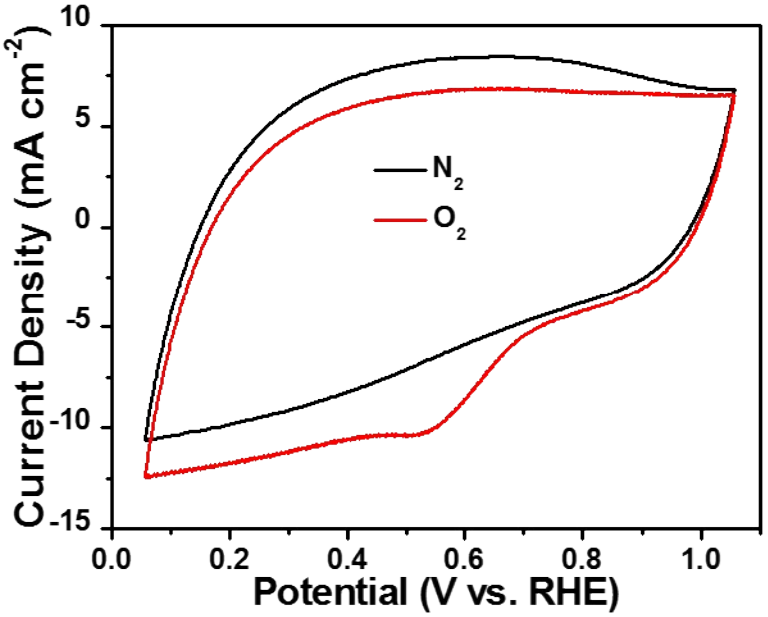

Figure S15. The CV curves of Co@SNHC in acidic conditions.

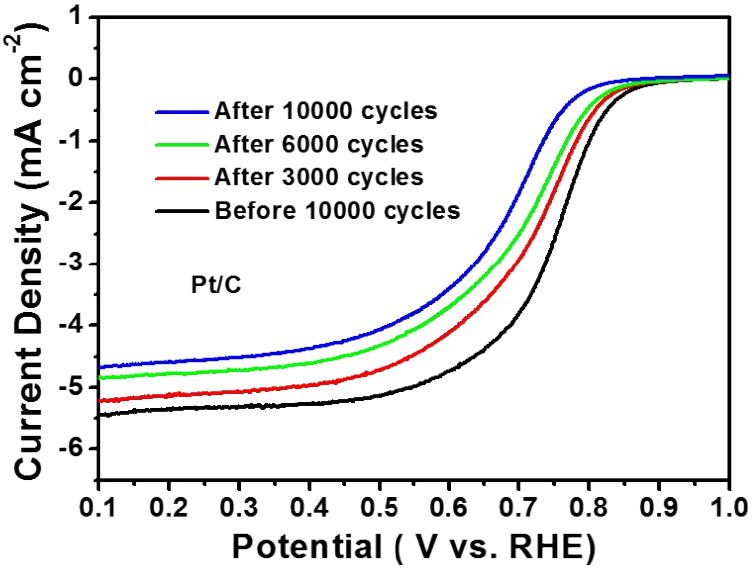

Figure S16. LSV polarization curves (1,600 rpm) of Pt/C before and after 3,000, 6,000 and 10,000 cycles in 0.1 M $HClO_4$.

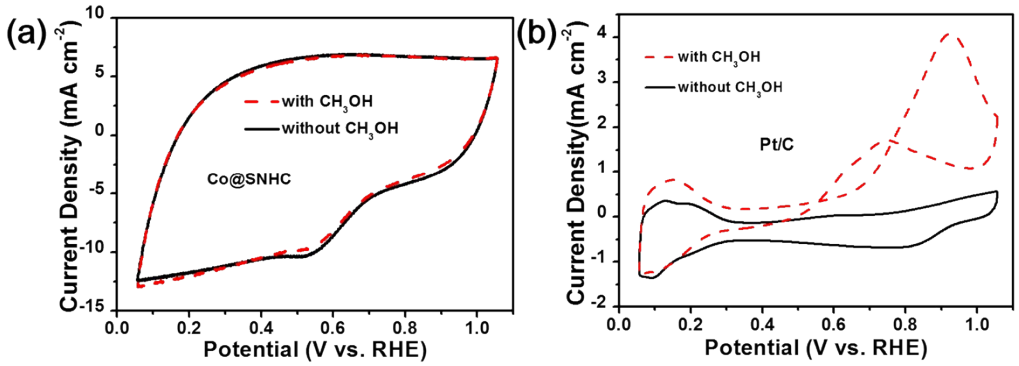

Figure S17. CV polarization curves of (a) Co@SNHC and (b) Pt/C in O_2-saturated 0.1 M $HClO_4$ solution with or without 1 M CH_3OH.

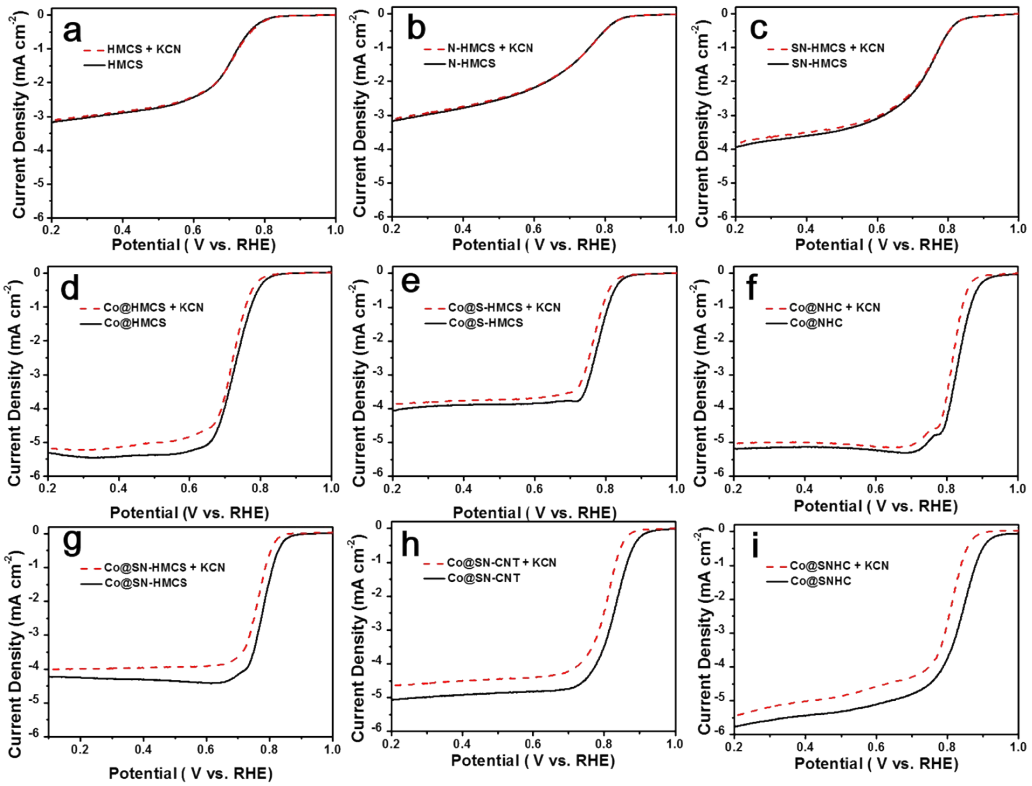

Figure S18. LSV curves of HMCS (a), N-HMCS (b), SN-HMCS (c), Co@HMCS (d), Co@S-HMCS (e), Co@NHC (f), Co@SN-HMCS (g), Co@SN-CNT (h) and Co@SNHC (i) without and with 5 mmol CN^- in 0.1 M KOH.

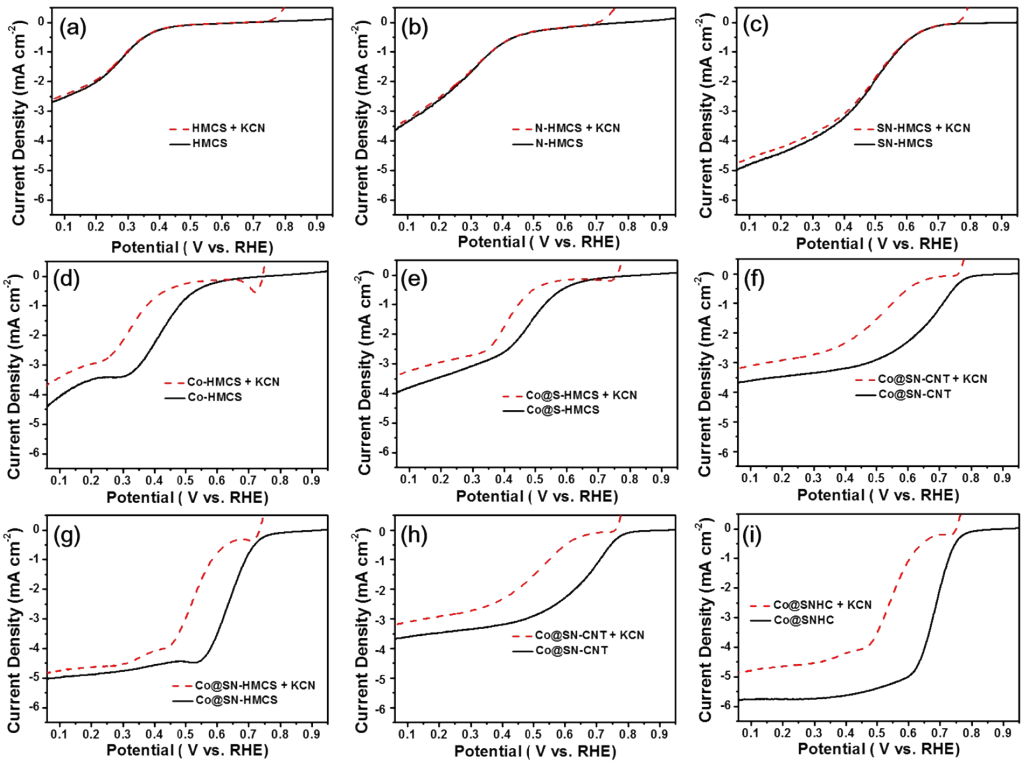

Figure S19. LSV curves of HMCS (a), N-HMCS (b), SN-HMCS (c), Co@HMCS (d), Co@S-HMCS (e), Co@NHC (f), Co@SN-HMCS (g), Co@SN-CNT (h) and Co@SNHC (i) without and with 5 mmol CN^-in 0.1 M $HClO_4$.

Table S1. X-ray photoelectron spectroscopy results for the HMCS, N-HMCS, SN-HMCS, Co@SN-CNT, Co@SN-HMCS, Co@NHC and Co@SNHC catalysts.

Sample	metal content [at.%]	C content [%]	N content [%]	S content [%]
HMCS	0	100	0	0
N-HMCS	0	79.26	20.74	0
SN-HMCS	0	79.68	19.68	0.64
Co@SN-CNT	1.44	86.9	10.71	0.94
Co@SN-HMCS	0.59	78.71	20.04	0.66
Co@NHC	1.23	79.45	19.32	0
Co@SNHC	1.62	76.86	20.57	0.95

Table S2. Energy-dispersive x-ray spectroscopy results for the HMCS, N-HMCS, SN-HMCS, Co@SN-CNT, Co@SN-HMCS, Co@NHC and Co@SNHC catalysts.

Sample	metal content [at.%]	C content [%]	N content [%]	S content [%]
HMCS	0	100	0	0
N-HMCS	0	78.38	21.62	0
SN-HMCS	0	78.66	20.51	0.83
Co@SN-CNT	2.24	78.72	19.28	1.33
Co@SN-HMCS	0.76	77.8	20.53	0.91
Co@NHC	2.05	78.27	19.68	0
Co@SNHC	2.62	75.36	20.57	1.45

Table S3. Thermogravimetric (TGA) and atomic absorption spectroscopy (AAS) results for Co@SN-CNT, Co@SNHC, Co@NHC and Co@SN-HMCS catalysts.

	Co@SN-CNT Co wt%	Co@SNHC Co wt%	Co@NHC Co wt%	Co@SN-HMCS Co wt%
TG	21.2	19.3	17.3	10.2
AAS	18.3	15.2	14.3	8.4

The atomic/weight ratios of as-synthesized electrocatalysts were measured by AAS, TG, XPS and EDX as shown in **Table S1-3**. The atomic ratio of Co, C, N and S of these as-synthesized catalysts obtained from XPS and EDX, as summarized in **Table S1** and **Table S2**. Except HMCS, the atomic ratio of N in other materials are nearly 20 at%. The atomic ratio of S atom in SN-HMCS, Co@SN-CNT, Co@SNHC and Co@SN-HMCS are nearly 1 at%. The results show that the doping amount of nitrogen and sulfur is similar in this system. According to the XPS results, the Co metal atomic ratio of Co@SN-CNT, Co@SNHC, Co@NHC and Co@SN-HMCS is 1.62 at%, 1.44 at%, 1.23 at% and 0.59 at%, respectively. In the EDX tests, atomic ratio of Co is similar to XPS results. The XPS and EDX only measure metal content on the surface of materials. The TG analyzer and AAS further detect Co weight ratio. As show in the **Table S3**, the weight ratio of Co atom of Co@SN-CNT is slightly more than that of Co@SNHC. However, Co@SNHC exhibited higher ORR activity than that Co@SN-CNT in alkaline and acidic medium. This phenomenon suggested that advantages of the 3D hybrid nanostructure with strongly coupled Co@SN-HMCS and Co@SN-CNT on improving ORR activities, whereas the Co@SN-HMCS brings catalytic activity due to the easy access to the active sites and the improved mass-transport properties as a mesoporous sphere structure. Additionally, the weight ratio of Co atom of Co@NHC is similar to Co@SNHC. However, Co@SNHC exhibited

higher ORR activity than that of Co@NHC in alkaline and acidic medium, indicated that the introduction of sulfur atom is play an important role in this work.

Table S4. ORR performance parameters of the as-prepared electrocatalysts derived from the RDE curves in 0.1 M KOH conditions.

Sample	E_{onset} (V)	$E_{1/2}$ (V)	J (mA cm^{-2}) (E at 0.4 V)
HMCS	0.825 V	0.722 V	-2.890
N-HMCS	0.845 V	0.730 V	-2.890
SN-HMCS	0.844 V	0.736 V	-3.683
Co@HMCS	0.864 V	0.731 V	-5.380
Co@S-HMCS	0.869 V	0.780 V	-4.652
Co@SN-CNT	0.967 V	0.826 V	-4.928
Co@SN-HMCS	0.906 V	0.780 V	-4.430
Co@NHC	0.931 V	0.806 V	-4.980
Co@SNHC	0.990 V	0.831 V	-5.511

Table S5. Comparison of the electrochemical activity of Co@SNHC with previously reported ORR catalysts in alkaline and acidic conditions.

Catalysts	onset potential (V vs. RHE)	$E_{1/2}$ (V vs. RHE)	electrolyte	Reference
Co@SNHC	**1.012 V**	**0.831 V**	**0.1 M KOH**	
		0.682 V	**0.1 M $HClO_4$**	in this work
(Fe, Co) NCs	0.91 V	0.85 V	**0.1 M KOH**	[S2]
Co_9S_8/N, S-DLCTs	0.927 V	0.89 V	**0.1 M KOH**	[S3]
Co-CoO/N-rGO	0.88 V	0.78 V	**0.1 M KOH**	[S4]
Co_9S_8/NHCS	0.97 V	0.86 V	**0.1 M KOH**	
	0.82 V	0.62 V	**0.1 M $HClO_4$**	[S5]
$Co_{1-x}S$/RGO	0.87 V		**0.1 M KOH**	[S6]
N-CG-CoO	0.90 V	0.81 V	**0.1 M KOH**	[S7]

$NiCo_2O_4$@N/S-rGO	0.92 V	0.79 V	**0.1 M KOH**	[S8]
NCNT/$Co_{0.51}Mn_{0.49}O$	0.96 V	0.84 V	**0.1 M KOH**	[S9]
CoS_2/N,S-GO	0.97 V	0.79 V	**0.1 M KOH**	[S10]
NC@Co-NGCDSNC	0.920 V	0.820 V	**0.1 M KOH**	[S11]
$Co_3FeS_{1.5}(OH)_6$	0.721 V	0.680 V	**0.1 M $HClO_4$**	[S12]
NS/rGO-Co	0.970 V	0.820 V	**0.1 M KOH**	[S13]
Co_9S_8/C	0.955 V	0.818 V	**0.1 M KOH**	[S14]

Table S6. ORR performance parameters of as-prepared electrocatalysts derived from

Sample	E_{onset} (V)	$E_{1/2}$ (V)	J (mA cm^{-2}) (E at 0.5 V)
N-HMCS	0.576 V	0.328 V	-0.06
SN-HMCS	0.755 V	0.465 V	-1.87
Co@HMCS	0.640 V	0.369 V	-0.74
Co@S-HMCS	0.698 V	0.457 V	-1.39
Co@SN-HMCS	0.787 V	0.631 V	-4.20
Co@SN-CNT	0.789 V	0.668 V	-0.50
Co@NHC	0.797 V	0.618 V	-2.54
Co@SNHC	0.852 V	0.682 V	-5.53

RDE curves in 0.1 M $HClO_4$ conditions.

Table S7. Zn-air batteries performance of some previous literature of nonprecious metal or nonmetal catalysts.

Air catalysts	Electrolytes	Open circuit potential	Power density	Specific capacity	Durability	Ref.
Co@SNHC	6M KOH	1.48 V	105 mW cm^{-2}	708.0 mAh g^{-1}	72 h	Our work
Fe/Co-N/S-C	6M KOH	1.395 V	102.63mW cm^{-2}	NA	26.7 h	[S15]
S,N-Fe/N/C-CNT	6M KOH	1.35 V	102.7 mW cm^{-2}	NA	100 h	[S16]
FeCo@MNC	6M KOH	1.41 V	143 mW cm^{-2}	NA	48 h	[S17]
$FeCoO_x$/NrGO	6M KOH	1.40 V	86 mW cm^{-2}	735 mAh g^{-1}	120 h	[S18]
MOF(Co)/C(3:1)-500	6M KOH	1.43 V	91 mW cm^{-2}	620 mAh g^{-1}	5.7 h	[S19]
$NiCo_2S_4$/N-CNT	6M KOH	1.49 V	147 mW cm^{-2}	431.0 mAh g^{-1}	16.7 h	[S20]
NiO/CoN	6M KOH	1.46 V	79.6 mW cm^{-2}	690.0 mAh g^{-1}	8.3 h	[S21]
HPC-900	6M KOH	1.50 V	NA	647.0 mAh g^{-1}	110 h	[S22]
nNiFe LDH/3D MPC	6M KOH	1.51 V	97 mW cm^{-2}	537.0 mAh g^{-1}	NA	[S23]

Reference:

[S1] S. Feng, W. Li, Q. Shi, Y. Li, J. Chen, Y. Ling, A. Asiri, D.Y. Zhao, Chem. Commun., 2014, **50**, 329–331.

[S2] J.B. Xi, Y.T. Xia, Y.Y. Xu, J.W. Xiao, S. Wang, 2015, DOI: 10.1039/c5cc03946k.

[S3] C.C. Hu, J. Liu, J. Wang, W.X. She, J.W. Xiao, J.B. Xi, Z.W. Bai and S. Wang, *ACS Appl. Mater. Interfaces*, 2018, **10**, 33124–33134.

[S4] X. Liu, W. Liu, M. Ko, M. Park, M. Kim, P. Oh, S. Chae, S. Park, A. Casimir, G. Wu and J. Cho, *Adv. Funct. Mater.*, 2015, **25**, 5799.

[S5] J. Wang, L.Q. Li, X. Chen, Y.L. Lu and W.S. Yang, *J. Mater. Chem. A*, 2016, **4**, 11342–11350.

[S6] H. L. Wang, Y. Y. Liang, Y. G. Li, and H J. Dai, *Angew. Chem. Int. Ed.*, 2011, **50**, 10969–10972.

[S7] S. Mao, Z. Wen, T. Huang, Y. Hou and J. Chen, *Energy Environ. Sci.*, 2014, **7**, 609.

[S8] Q. Liu, J. T. Jin and J. Y. Zhang, *ACS Appl. Mater. Interfaces*, 2013, **5**, 5002–5008.

[S9] X. Liu, M. Park, M. Kim, S. Gupta, X. Wang, G. Wu and J. Cho, *Nano Energy*, 2016, **20**, 315.

[S10] P. Ganesan, M. Prabu, J. Sanetuntikul and S. Shanmugam, *ACS Catal.*, 2015, **5**, 3625–3637.

[S11] S. H. Liu, Z. Y. Wang, S. Zhou, F. J. Yu, M. Z. Yu, C. Y. Chiang, W. Z. Zhou, J. J. Zhao and J. S. Qiu, *Nano Energy*, 2017, **31**, 541–550.

[S12] H.F. Wang, C. Tang, B. Wang, B.Q. Li and Q. Zhang, *Adv. Mater.*, 2017, **29**, 1702327.

[S13] N. Wang, L. G. Li, D.K. Zhao, X. W. Kang, Z. H. Tang, S. W. Chen, *Small*, 2017, **13**, 1701025.

[S14] Z. Zhou, A. Chen, X. Fan, A. Kong, Y. Shan, *Electrochim. Acta*, 2018, **265**, 32–40.

[S15] C. H. Li, H. X. Liu, Z. Y. Yu, *Appl. Catal. B*, 2019, **241**, 95–103.

[S16] P. Z. Chen, T. P. Zhou, L. L. Xing, K. Xu, Y. Tong, H. Xie, L. D. Zhang, W. S. Yan, W. S. Chu, C. Z. Wu and Y. Xie, *Angew. Chem. Int. Ed.*, 2017, **129**, 625–629.

[S17] C. L. Li, M. C. Wu and R. Liu, *Appl. Catal. B*, 2019, **244**, 150–158.

[S18] L. Wei, H. E. Karahan, S. L. Zhai, H. W. Liu, X. C. Chen, Z. Zhou, Y. J. Lei, Z. W. Liu and Y. Chen, *Adv. Mater.*, 2017, **29**, 1701410–1701420.

[S19] X. R. Yia, X. B. He, F. X. Yin, B. H. Chen, G. R. Li and H. Q. Yin, *Electrochim. Acta*, 2019, **295**, 966–977.

[S20] X. P. Han, X. Y. Wu, C. Zhong, Y. D. Deng, N. Q. Zhao and W. B. Hu, *Nano Energy*, 2017, **31**, 541–550.

[S21] J. Yin, Y. X. Li, F. Lv, Q. H. Fan, Y. Q. Zhao, Q. L. Zhang, W. Wang, F. Y. Cheng, P. X. Xi and S. J. Guo, *ACS Nano*, 2017, **11**, 2275–2283.

[S22] W. H. Niu, L. G. Li, N. Wang, S. B. Zeng, J. Liu, D. K. Zhao and S. W. Chen, *J.*

Mater. Chem. A, 2016, **4**, 10820–10827.

[S23] W. Wang, Y. C Liu, J. Li, J. Luo, L. Fu and S. L. Chen, *J. Mater. Chem. A*, 2018, **6**, 14299–14306.